Malaysian Journal of Mathematical Sciences 16(3): 391–411 (2022)
https://doi.org/10.47836/mjms.16.3.01

Malaysian Journal of Mathematical Sciences

Journal homepage: https://einspem.upm.edu.my/journal

Numerical Simulations of the Fractional-Order SIQ Mathematical Model of Corona Virus Disease Using the Nonstandard Finite Difference Scheme

Raza, N.*[1], Bakar, A.[1], Khan, A.[1], and Tunç, C.[2]

[1]*Department of Mathematics, University of the Punjab, Quaid-e-Azam Campus, Pakistan*
[2]*Department of Mathematics, Faculty of Sciences, Van Yuzuncu Yil University, 65080, Campus, Van-Turkey Turkey*

E-mail: cemtunc@yahoo.com
**Corresponding author*

Received: 30 June 2022
Accepted: 10 August 2022

Abstract

This paper proposes a novel nonlinear fractional-order pandemic model with Caputo derivative for corona virus disease. A nonstandard finite difference (NSFD) approach is presented to solve this model numerically. This strategy preserves some of the most significant physical properties of the solution such as non-negativity, boundedness and stability or convergence to a stable steady state. The equilibrium points of the model are analyzed and it is determined that the proposed fractional model is locally asymptotically stable at these points. Non-negativity and boundedness of the solution are proved for the considered model. Fixed point theory is employed for the existence and uniqueness of the solution. The basic reproduction number is computed to investigate the dynamics of corona virus disease. It is worth mentioning that the non-integer derivative gives significantly more insight into the dynamic complexity of the corona model. The suggested technique produces dynamically consistent outcomes and excellently matches the analytical works. To illustrate our results, we conduct a comprehensive quantitative study of the proposed model at various quarantine levels. Numerical simulations show that can eradicate a pandemic quickly if a human population implements obligatory quarantine measures at varying coverage levels while maintaining sufficient knowledge.

Keywords: corona virus disease; Caputo fractional derivative; basic reproduction number; local stability; nonstandard finite difference method.

1 Introduction

Corona virus disease (COVID-19) is a deadly global epidemic with an unusual high mortality rate due to the infectious respiratory virus SARS-CoV-2. This virus speards consistently across individuals and affects the people all over the globe. In the Chinese city of Wuhan, the first attack of the Corona virus disease occurred around the end of December 2019. It proliferates in many regions of China before spreading globally to almost 223 Asian, Australian, American and European nations [18, 17, 50]. By February 11, 2022, the World Health Organization (WHO) registered that there would be over 404, 910, 528 confirmed cases and 5, 783, 776 loss of lives worldwide. It is surprising that the WHO has recorded 2, 473, 605 new cases to date, although verified cases have risen. However, about 333, 032, 099 persons have been rescued from COVID-19. By February 06, 2022, total of 10, 095, 615, 243 vaccination doses had been given out [34]. The USA, India, Brazil and France are now the countries with the largest number of positive cases.

The current evidence shows that the respiratory droplets produced by an infected person's sneezing, coughing and spitting are the primary routes of Corona virus transmission among the people [16, 38, 25]. Healthcare workers might get infected while treating Corona patients. Every person may get highly sick or die from a Corona infection at any age and any moment. People over the age of 60 and those suffering from serious illnesses such as cardiovascular disease, obesity, tumors, diabetes or respiratory problems are at a higher risk of becoming extremely sick with the Corona virus. They may remain infectious for a more extended period. Without requiring hospitalization, around 5% of people who have symptoms will become severely ill and need special attention, approximately 80% will get over the viral infection and approximately 15% will become highly unwell and require oxygen [32]. If the pandemic is not controlled, the virus can be spread on a vast scale. As a result, it is unavoidable to adopt extensive preventative measures while caring for infected individuals.

Computational mathematical techniques are used to model the infections among populations quantitatively [40, 3]. In the last few decades, mathematical models of infectious disease dynamics have been developed. The most frequent mathematical formulations depict the individual transition in a community between the compartments, reflecting the scenario of individual infection with astonishing precision. These compartmental disease models divide a population into categories based on the infectious status of each person and the growth of the whole population has been simulated over time. Since the emergence of COVID-19, numerous researchers have developed and used these models to investigate the dynamical behavior of a Corona virus disease [13, 29, 24, 5, 47, 31, 54, 19]. These research studies used mathematical models based on integer-order derivatives with specific limits on the order of the derivatives. The main objective was to learn more about the pandemic's transmission, spread, effect, prevention and control mechanisms. It is essential to formulate an accurate and efficient mathematical analysis of these models in epidemiology. It is always beneficial to design a technique to restrict the disease's spread in the future.

Several researchers have turned to fractional calculus to overcome these limitations, a relatively new branch of mathematics. Fractional-order differential operators are used in fractional calculus to explain a range of natural occurrences, truths and facts with nonlocal dynamics and strange behavior. Because such frameworks depend on the memory strength controlled by order of a fractional derivative [48, 35, 27, 23, 51, 28]. Several academics have recently discovered and proposed efficient strategies for determining accurate and approximate solutions to the differential equations containing fractional operators. Many researchers are looking at the epidemic models employing fractional operators for various infectious diseases because they exhibit a plausible biphasic reduction in disease contamination [37, 7, 4]. These fractional operators each have their own set of advantages and disadvantages. Fractional-order conditions are required for Riemann-Liouville fractional operators to solve mathematical models. The Caputo operator overcomes this limitation and the initial conditions with integer-order derivatives with physical relevance may be used with the Caputo fractional operator [42, 11, 2].

The basic model of Kermack and McKendrick [33, 14] is used in most of the COVID-19 mathematical models that simulate the dynamics of infectious diseases among a community of humans. This model subdivides the population into three compartments, i.e, susceptible people S, who are not affected but at risk of being infected; infectious people I, who are infected and capable of spreading the disease to others and removed people R, who have recovered or died from the disease. This basic model [14] is often known as the SIR model which has effectively predicted several epidemics, including the Influenza outbreak at the school of England in 1978 and the plague India in 1905. With the reformulation of this model, more contemporary disease outbreaks have been modelled, including the SARS epidemic [55], the H5N1 Influenza [15], the H1N1 Influenza [22] and the Ebola outbreak [10]. The Kermack-McKendrick model is being used in this study and the reason is that the dynamics of COVID-19 in the population are comparable to the behavior of Influenza. We want to explore the quarantine's impact on the COVID-19 population. The quarantine effect is highlighted since it is easier to control than any other factor. The infection rate has the most significant impact on disease transmission dynamics, yet it is challenging to manage. The second component is the recovery rate, which we can not maintain in COVID-19 since people's immunity mainly determines it. The government may impose the quarantine rate forcefully, allowing it to be adequately monitored and overseen. No dought, vaccination does indeed have a powerful effect on an outbreak. However, we do not include it in our model since we are primarily interested in simulating the early phase of an epidemic before vaccine manufacturing.

This study extends the continuous integer-order model to fractional-order and transforms it into a discrete model using the NSFD numerical approach [8, 20, 1]. We anticipate our projected SIQ fractional model for the dynamical qualities. It has been determined that most classic standard approaches may become unbounded divergent when applied to a nonlinear system. As the temporal grid size expanded, these numerical approaches led to negative solutions, severe oscillations, breakups, disorder and solutions not converging to the true steady states. As a result, developing the NSFD technique is the most effective way to solve our fractional model. Completing a full numerical analysis of the suggested model will show that the devised scheme is dynamically consistent. Besides, for some scientific works on a fractional order Zika virus model, fractional-order six-neuron bi-directional associative memory neural network, the dynamics of Leptospirosis disease, the diseases in the prey population, the tuberculosis and qualitavie behaviors of diffrential equations of second and third order , we referee the readers to the papers in [9, 49, 21, 39, 41, 43, 44, 45, 52, 53].

The paper is organized as follows. Section 2 outlines the development of the suggested compartmental model. The proposed Corona model is described in fractional form is given in Section 3. Section 4 briefly explains the features of the proposed fractional model and some fixed point theorems are given in this Section. Section 5 comprises the proofs of the positivity and boundedness of the solutions. Equilibrium points and the threshold parameter $\mathcal{R}_\circ$ for the proposed fractional model are computed in Sections 6 and 7, respectively. Section 8 proved that the model's equilibrium points are locally asymptotically stable. To approximate the fractional model's solution, we developed the NSFD numerical technique and numerically analyzed the suggested fractional model in Section 9. The summary of our results is given in Section 10.

2 The Integer-Order COVID-19 Model

In epidemiology, nonlinear models describe the transmission dynamics of the deadly Corona virus among a community of humans. Several mathematical models in the literature have been used with different assumptions based on how the Corona virus epidemic spreads. This section investigates novel real-world integer order SIQ model [6] of the Corona epidemic for the Saudi Arabia population data. We investigate a three-dimensional model with three subpopulations, i.e, susceptible population $S(t)$, infected population $I(t)$ and quarantined population $Q(t)$. The population is homogeneously mixed and disease spreads through direct contact between susceptible and infected people.

Therefore, the COVID-19 SIQ epidemic model is obtained which is described by a system of differential equations as follows

$$\begin{aligned} \frac{dS}{dt} &= \Pi - \beta \frac{SI}{N} - \mu_1 S, \\ \frac{dI}{dt} &= \beta \frac{SI}{N} - (\delta + \alpha_1 + \mu_1 + \mu_2) I, \\ \frac{dQ}{dt} &= \delta I - (\alpha_2 + \mu_2 + \mu_1) Q, \end{aligned} \tag{1}$$

where $N(t)$ represents the overall population in the region under examination at any given time t, which is the sum of all the three subpopulations. Its transmission coefficient is represented by β. Here, Π and μ_1 denotes the total birth rate and the per-capita death rate from causes other than COVID-19 respectively. Furthermore, the per-capita rate of mortality from COVID-19 is μ_2. We also consider the proportion of infected patients who are found and admitted to quarantine either at home or at a health care institution as δ and the average period from infection to quarantine admission is $1/\delta$. The per-capita recovery rate from COVID-19 is α_1 for patients who are not in quarantine and α_2 for those who are.

It is assumed that all of the parameters associated with the system (1) are strictly positive and the initial conditions are non-negative. Table **1** shows the model parameter values as well as the initial conditions employed in the numerical results.

3 COVID-19 Model in Caputo Sense

We begin by recalling some basic concepts coresponding to the Caputo and Atangana-Baleanu fractional operators [36].

Definition 3.1. *Let ρ be a positive real integer with the $n-1 < \rho \leq n$, for $n \in \mathbb{N}$. The Caputo fractional derivative of the function $\zeta(t)$ of order ρ is defined by*

$$ {}^{C}D_t^{\rho}\zeta(t) = \frac{1}{\Gamma(n-\rho)} \int_0^t \frac{\zeta^{(n)}(t)(t-\omega)^{n-\rho}}{(t-\omega)} d\omega, \tag{2}$$

where $\zeta^{(n)}(t) = \frac{d^n\zeta(t)}{dt^n}$. When $0 < \rho \leq 1$, the Caputo fractional derivative of order ρ reduces to

$$ {}^{C}D_t^{\rho}\zeta(t) = \frac{1}{\Gamma(1-\rho)}\int_0^t \frac{\zeta^{'}(t)(t-\omega)^{\rho}}{(t-\omega)}d\omega. \tag{3} $$

Clearly, ${}^{C}D_t^{\rho}\zeta(t)$ tends to $\zeta^{'}(t)$ whenever ρ tends to 1.

Definition 3.2. *The definition of the associated integral with $\rho > 0$ is given by*

$$ I_t^{\rho}\zeta(t) = \frac{1}{\Gamma(\rho)}\int_0^t \frac{\zeta(t)(t-\omega)^{\rho}}{(t-\omega)}d\omega, \quad 0 < \rho \leq 1, t > 0. \tag{4} $$

Definition 3.3. *The fractional operator Atangana-Baleanu-Caputo (ABC) with $\rho \in (0, 1]$ is defined as follows*

$$ {}_{a}^{ABC}D_t^{\rho}\zeta(t) = \frac{ABC(\rho)}{(1-\rho)}\int_a^t \zeta^{'}(t)E_{\rho}\Big[-\rho\frac{(t-\omega)^{\rho}}{(1-\omega)}\Big]d\omega. \tag{5} $$

Definition 3.4. *The definition of the associated ABC fractional integral with $\rho > 0$ is expressed as*

$$ {}_{a}^{ABC}I_t^{\rho}\zeta(t) = \frac{(1-\rho)}{B(\rho)}\zeta(t) + \frac{\rho}{B(\rho)\Gamma(\rho)}\int_a^t \frac{\zeta(t)(t-\omega)^{\rho}}{(t-\omega)}d\omega, \quad \rho \in (0, 1]. \tag{6} $$

To investigate the memory effects and learn more about the epidemic, we reformulate the model (1) with a Caputo fractional derivative. Therefore, we obtain the fractional-order COVID-19 model in the Caputo operator as

$$ \begin{aligned} {}^{C}D_t^{\rho}S(t) &= \Pi - \beta\frac{SI}{N} - \mu_1 S, \\ {}^{C}D_t^{\rho}I(t) &= \beta\frac{SI}{N} - (\delta + \alpha_1 + \mu_1 + \mu_2)I, \\ {}^{C}D_t^{\rho}Q(t) &= \delta I - (\alpha_2 + \mu_2 + \mu_1)Q, \end{aligned} \tag{7} $$

for $t \geq 0$ and $\rho \in (0, 1]$. The epidemiological region G for the proposed system (7) can be defined as

$$ G = \Big\{ (S(t), I(t), Q(t)) \in \mathbb{R}_+^3 : 0 < N(t) \leq \frac{\Pi}{\mu_1},\ S(t), I(t), Q(t) \geq 0 \Big\}. \tag{8} $$

4 Existence and Uniqueness of Solution

This section looks at the existence and uniqueness of the solution for the fractional model. The following are the sufficient conditions for the existence and uniqueness of a solution [11, 26].

Theorem 4.1. *The fractional model (7) has a unique solution for each non-negative initial condition.*

Proof. We are looking for a sufficient condition in the region $G \times (0, T]$ to ensure the existence and uniqueness of the solution of fractional-order system, where

$$ G = \Big\{ (S, I, Q) \in \mathbb{R}_+^3; \max(|S|, |I|, |Q|) \leq M \Big\}. $$

The strategy employed in [11] is applied. Consider the following mapping

$$\Psi(\eta) \;=\; \left(\Psi_1(\eta), \Psi_2(\eta), \Psi_3(\eta)\right),$$

and

$$\begin{aligned}
\Psi_1(\eta) &= \Pi - \beta\frac{SI}{N} - \mu_1 S,\\
\Psi_2(\eta) &= \beta\frac{SI}{N} - (\delta + \alpha_1 + \mu_1 + \mu_2)I,\\
\Psi_3(\eta) &= \delta I - (\alpha_2 + \mu_1 + \mu_2)Q.
\end{aligned} \tag{9}$$

We denote $\eta = (S, I, Q)$ and $\bar{\eta} = (\bar{S}, \bar{I}, \bar{Q})$. For any $\eta, \bar{\eta} \in G$, it follows from (9) that

$$\|\Psi(\eta) - \Psi(\bar{\eta})\| = |\Psi_1(\eta) - \Psi_1(\bar{\eta})| + |\Psi_2(\eta) - \Psi_2(\bar{\eta})| + |\Psi_3(\eta) - \Psi_3(\bar{\eta})|. \tag{10}$$

After some simplification (10) can be written as

$$\begin{aligned}
\|\Psi(\eta) - \Psi(\bar{\eta})\| = &\left| -\mu_1(S - \bar{S}) - \frac{\beta}{N}(SI - \bar{S}\bar{I})\right| + \left|\frac{\beta}{N}(SI - \bar{S}\bar{I}) - (\delta + \alpha_1 + \mu_1 + \mu_2)(I - \bar{I})\right| \\
&+ |\delta(I - \bar{I}) - (\alpha_2 + \mu_1 + \mu_2)(Q - \bar{Q})|,
\end{aligned}$$

which then becomes

$$\|\Psi(\eta) - \Psi(\bar{\eta})\| \;\leq\; H_1|S - \bar{S}| + H_2|I - \bar{I}| + H_3|Q - \bar{Q}|, \tag{11}$$

$$\|\Psi(\eta) - \Psi(\bar{\eta})\| \;\leq\; \varphi\|\eta - \bar{\eta}\|, \tag{12}$$

where

$$H_1 = \mu_1 + \frac{2M\beta}{N}, \quad H_2 = \frac{2M\beta}{N} + 2\delta + \alpha_1 + \mu_1 + \mu_2, \quad H_3 = \alpha_2 + \mu_1 + \mu_2,$$

and

$$\varphi \;=\; \max\{H_1, H_2, H_3\}.$$

Therefore, $\Psi(\eta)$ fulfills the Lipschitz condition with respect to η. Thus, there exists a unique solution $\eta(t)$ of the system (7) with the initial condition $\eta^\circ = (S^\circ, I^\circ, Q^\circ)$ [26]. Hence, the existence and uniqueness of the solution of the proposed fractional model are established. □

Theorem 4.2. *There exists a unique solution $\eta(t) \in G$ of the model (7) with initial condition η°, for each $\eta^\circ = (S^\circ, I^\circ, Q^\circ)$, $\forall\, t \geq 0$.*

5 Non-Negativity and Boundedness

In this section, we are interested in non-negative and bounded solutions of the fractional model (7) due to their biological importance. The following result ensures that the solutions of the fractional model are non-negative and bounded.

Theorem 5.1. *Every solution of the proposed fractional model (7) that begin in $\mathbb{R}^3_+$ is non-negative and uniformly bounded.*

Proof. We follow the approach used by [11], to prove the boundedness of the solution of the fractional model. Consider, $N(t) = S(t) + I(t) + Q(t)$ is a function and for each $\mu_1 > 0$, we have

$$\begin{aligned} {}^C D_t^\rho N(t) + \mu_1 N(t) &= {}^C D_t^\rho S(t) +^C D_t^\rho I(t) +^C D_t^\rho Q(t) + \mu_1 N(t) \\ &= \Pi - \mu_1 S(t) - (\alpha_1 + \mu_1 + \mu_2) I(t) - (\alpha_2 + \mu_1 + \mu_2) Q(t) + \mu_1 N(t) \\ &= \Pi - (\alpha_1 + \mu_2) I(t) - (\alpha_2 + \mu_2) Q(t) \\ &\leq \Pi. \end{aligned} \tag{13}$$

Using Lemma 9 from [12], then the inequality (13) becomes

$$N(t) \leq N(0) E_{\rho,1}(-\mu_1 t^\rho) + \Pi t^\rho E_{\rho,\rho+1}(-\mu_1 t^\rho), \tag{14}$$

where $E_{\rho,1}$ is a function called the Mittag-Leffler. Using Lemma 5 and Corollary 6 in [12], then inequality (14) becomes

$$N(t) \leq \frac{\Pi}{\mu_1}, \quad t \to +\infty. \tag{15}$$

Consequently, all the solutions of proposed fractional model (7) starting in $\mathbb{R}^3_+$ are restricted to the feasible region G, where

$$G = \left\{ (S(t), I(t), Q(t)) \in \mathbb{R}^3_+ : N(t) \leq \frac{\Pi}{\mu_1} \right\}. \tag{16}$$

Next, we prove that the non-negativity of the solutions of the fractional model. By the first equality of model (7), we have

$$\begin{aligned} {}^C D_t^\rho S(t) &= \Pi - \beta \frac{SI}{N} - \mu_1 S \\ &\geq -(\beta \frac{I}{N} - \mu_1) S \\ &\geq -(\mu_1) S \\ &\geq -C_1 S, \end{aligned} \tag{17}$$

where $C_1 = \mu_1$. Using Lemma 9 from [12] and $E_{\rho,1}(t) > 0$, for any $\rho \in (0, 1]$. So, the inequality (17) becomes

$$S(t) \geq S(0) E_{\rho,1}(-C_1 t^\rho) \Rightarrow S(t) \geq 0. \tag{18}$$

Using the second equality of the model (7), we have

$$\begin{aligned} {}^C D_t^\rho I(t) &= \beta \frac{SI}{N} - (\delta + \alpha_1 + \mu_1 + \mu_2) I \\ &= \left[\beta \frac{S}{N} - (\delta + \alpha_1 + \mu_1 + \mu_2) \right] I \\ &\geq -(\delta + \alpha_1 + \mu_1 + \mu_2) I \\ &\geq -C_2 I, \end{aligned} \tag{19}$$

where $C_2 = \delta + \alpha_1 + \mu_1 + \mu_2$. Therefore, the coresponding inequality (19) becomes

$$I(t) \geq I(0)E_{\rho,1}(-C_2 t^{\rho}) \Rightarrow I(t) \geq 0. \tag{20}$$

Using the third equality of the model (7), we have

$$\begin{aligned} {}^{C}D_t^{\rho} Q(t) &= \delta I - (\alpha_2 + \mu_1 + \mu_2)Q \\ &\geq -(\alpha_2 + \mu_1 + \mu_2)Q \\ &\geq -C_3 Q, \end{aligned} \tag{21}$$

where $C_3 = \alpha_2 + \mu_1 + \mu_2$. Therefore,

$$Q(t) \geq Q(0)E_{\rho,1}(-C_3 t^{\rho}) \Rightarrow Q(t) \geq 0. \tag{22}$$

Thus, the non-negative nature of the solutions of the proposed fractional model (7) has been shown. □

Therefore, the proposed fractional model (7) is mathematically well-posed as all the theorems have proved the existence, uniqueness, boundedness and non-negativity of the solutions of the model.

6 Equilibrium Points

The equilibrium points of the suggested fractional model are examined in this section. Corona-free and Corona-endemic are the two types of equilibrium points for the considered model. To get these points, we set the right-hand side of the system (7) equal to zero as

$${}^{C}D_t^{\rho} S(t) = {}^{C}D_t^{\rho} I(t) = {}^{C}D_t^{\rho} Q(t) = 0,$$

which implies that

$$\begin{aligned} \Pi - \beta\frac{SI}{N} - \mu_1 S &= 0, \\ \beta\frac{SI}{N} - (\delta + \alpha_1 + \mu_1 + \mu_2)I &= 0, \\ \delta I - (\alpha_2 + \mu_1 + \mu_2)Q &= 0. \end{aligned}$$

Assuming that P° represents Corona-free equilibrium and P^{*} represents Corona-endemic equilibrium. For Corona-free equilibrium, $I^{\circ} = Q^{\circ} = 0$, then $\Pi - \mu_1 S^{\circ} = 0$ and $S^{\circ} = \Pi/\mu_1$. Thus, P° for the proposed fractional model is

$$P^{\circ}(S^{\circ}, I^{\circ}, Q^{\circ}) = P^{\circ}\left(\frac{\Pi}{\mu_1}, 0, 0\right)$$

and Corona-endemic equilibrium point $P^*(S^*, I^*, Q^*)$ is given by:

$$\begin{aligned} S^* &= \frac{1}{\mu_1}\left[\Pi - \frac{\beta I^*}{\mathcal{R}_0}\right] > 0, \\ I^* &= \frac{\Pi\mathcal{R}_0(1 - 1/\mathcal{R}_0)}{\beta(1 - 1/\mathcal{R}_0) + \mu_1 + \mu_1\delta/(\alpha_2 + \mu_1 + \mu_2)} > 0, \\ Q^* &= \frac{\delta I^*}{\alpha_2 + \mu_1 + \mu_2} > 0, \end{aligned}$$

in the epidemiological region G.

7 The Basic Reproduction Number $\mathcal{R}_\circ$

In this part, we use the next-generation matrix approach to determine the basic reproduction number $\mathcal{R}_\circ$ for the suggested fractional model (7). In compact form, the reduced system is expressed as follows

$$^{C}D_t^{\rho}\psi = \mathcal{P}(\psi) - \mathcal{Q}(\psi),$$

where $\psi = (I, Q)$.

$$\mathcal{P}(I,Q) = \begin{bmatrix} \frac{\beta SI}{N} \\ 0 \end{bmatrix}, \quad \mathcal{Q}(I,Q) = \begin{bmatrix} -(\delta + \alpha_1 + \mu_1 + \mu_2)I \\ \delta I - (\alpha_2 + \mu_1 + \mu_2)Q \end{bmatrix}.$$

The Jacobian matrices of $\mathcal{P}$ and $\mathcal{Q}$ at Corona-free equilibrium point P° are

$$J_{\mathcal{P}}(P^\circ) = \begin{bmatrix} \frac{\partial \mathcal{P}_1}{\partial I} & \frac{\partial \mathcal{P}_1}{\partial Q} \\ \frac{\partial \mathcal{P}_2}{\partial I} & \frac{\partial \mathcal{P}_2}{\partial Q} \end{bmatrix} = \begin{bmatrix} \frac{\beta\Pi}{\mu_1 N} & 0 \\ 0 & 0 \end{bmatrix},$$

$$J_{\mathcal{Q}}(P^\circ) = \begin{bmatrix} \frac{\partial \mathcal{Q}_1}{\partial I} & \frac{\partial \mathcal{Q}_1}{\partial Q} \\ \frac{\partial \mathcal{Q}_2}{\partial I} & \frac{\partial \mathcal{Q}_2}{\partial Q} \end{bmatrix} = \begin{bmatrix} -(\delta + \alpha_1 + \mu_1 + \mu_2) & 0 \\ \delta & -(\alpha_2 + \mu_1 + \mu_2) \end{bmatrix}.$$

Hence, the spectral radius ($\mathcal{R}_\circ$) of $J_{\mathcal{P}}(P^\circ)J_{\mathcal{Q}}^{-1}(P^\circ)$ for the proposed fractional model (7) is given as

$$\mathcal{R}_\circ = \frac{\beta\Pi}{\mu_1 N(\delta + \alpha_1 + \mu_1 + \mu_2)}. \tag{23}$$

8 Stability Analysis

This section discusses the stability of the fractional model (7) locally at both equilibrium points [37, 7].

8.1 Stability of the Corona-Free Equilibrium

Theorem 8.1. *The suggested fractional system's Corona-free equilibrium point P° is locally asymptotically stable if $\mathcal{R}_\circ < 1$ and unstable if $\mathcal{R}_\circ > 1$.*

Proof. For the fractional system (7), the Jacobian matrix at P° can be written as

$$\mathcal{J}(P^\circ) = \begin{bmatrix} -\mu_1 & -\frac{\beta\Pi}{\mu_1 N} & 0 \\ 0 & \frac{\beta\Pi}{\mu_1 N} - (\delta + \alpha_1 + \mu_1 + \mu_2) & 0 \\ 0 & \delta & -(\alpha_2 + \mu_1 + \mu_2) \end{bmatrix}. \tag{24}$$

Therefore, the eigenvalues of the matrix $\mathcal{J}(P^\circ)$ are

$$\lambda_1 = -\mu_1, \qquad \lambda_2 = -(\alpha_2 + \mu_1 + \mu_2), \qquad \lambda_3 = \frac{\beta\Pi}{\mu_1 N} - (\delta + \alpha_1 + \mu_1 + \mu_2). \tag{25}$$

The above Eq. (25) shows that $\lambda_1 = -\mu_1 < 0$ as $\mu_1 > 0$ and $\lambda_2 = -(\alpha_2 + \mu_1 + \mu_2) < 0$. As all the parameters are positive, i.e, α_2, μ_1 and $\mu_2 > 0$. From Eq. (25), λ_3 can be written as

$$\lambda_3 \quad = \quad (\delta + \alpha_1 + \mu_1 + \mu_2)[\mathcal{R}_\circ - 1].$$

Therefore,

$$\lambda_3 < 0 \Leftrightarrow \mathcal{R}_\circ < 1.$$

Thus, Corona free equilibrium point P° is LAS in the epidemiological region G and unstable when $\mathcal{R}_\circ > 1$. Hence, it is proved that the proposed system (7) at $P^\circ = (\frac{\Pi}{\mu_1}, 0, 0)$ is locally asymptotical stable for $\mathcal{R}_\circ < 1$ and unstable for $\mathcal{R}_\circ > 1$. □

8.2 Stability of the Corona-Endemic Equilibrium

Theorem 8.2. *If $\mathcal{R}_\circ > 1$, then the suggested fractional system (7) is considered to be LAS at Corona-endemic equilibrium point P^* but it is unstable for $\mathcal{R}_\circ < 1$.*

Proof. For the fractional system (7), the Jacobian matrix at P^* can be written as

$$\mathcal{J}(P^*) = \begin{bmatrix} p_{11} & p_{12} & 0 \\ p_{21} & p_{22} & 0 \\ 0 & p_{32} & p_{33} \end{bmatrix}, \tag{26}$$

where

$$p_{11} = \frac{\beta I_1}{N} - \mu_1, \qquad p_{12} = -\frac{\beta S_1}{N}, \qquad p_{21} = \frac{\beta I_1}{N}$$

and

$$p_{22} = \frac{\beta S_1}{N} - (\delta + \alpha_1 + \mu_1 + \mu_2), \qquad p_{32} = \delta, \qquad p_{33} = -(\alpha_2 + \mu_1 + \mu_2).$$

We have used Maple software to determine the eigenvalues of the Jacobian matrix $\mathcal{J}(P^*)$, given as

$$\lambda_1 = -(\alpha_2 + \mu_1 + \mu_2), \qquad \lambda_2 = \frac{(p_{11} + p_{22}) - \sqrt{\Delta}}{2}, \qquad \lambda_3 = \frac{(p_{11} + p_{22}) + \sqrt{\Delta}}{2}. \tag{27}$$

It is clear that

$$p_{11} + p_{22} < 0, \qquad \Delta = (p_{11} + p_{22})^2 - 4(p_{11}p_{22} - p_{12}p_{21}) > 0,$$

when $\mathcal{R}_\circ > 1$. From the above Eq. (27), $\lambda_1 = -(\alpha_2 + \mu_1 + \mu_2) < 0$ as α_2, μ_1 and $\mu_2 > 0$. From the preceding arguments, the remaining eigenvalues λ_2 and λ_3 must be negative. Hence, the proposed fractional system (7) at P^* is locally asymptotical stable, when $\mathcal{R}_\circ > 1$. □

9 Numerical Analysis

This part provides a numerical scheme and simulations to validate the theoretical results acquired in the preceding sections. The simulation is carried out with the help of MATLAB. We use the NSFD approach [46, 30] to obtain numerical results of the proposed fractional model for different values of ρ. Corona virus disease dynamic behavior throughout time (t) is modelled for the different values of fractional-order. Numerical simulations presented in this work are briefly explained.

Table 1: The initial conditions and numerical values of parameters [20].

S°	I°	Q°	Π	α_1	α_2	β	μ_1	μ_2
$34e+6$	1	0	1603	0.014	0.14	0.35	$4.62e-5$	0.012

9.1 NSFD Scheme and Simulations

The main purpose of this subsection is to provide a dynamically consistent numerical discrete framework for the proposed fractional system (7). It is important to note that all model variables and parameters are non-negative. To achieve a dynamically consistent discrete scheme, we must verify that the resultant discrete solutions are all non-negative, required to prevent scheme-dependent instabilities. The NSFD scheme should also meet the associated conservation law since the population is constant. These characteristics will be considered in the development of the numerical scheme.

We have used the algorithm, which is briefly explained in [46, 30]. Then discretize the suggested fractional model and we obtain

$$\sum_{i=0}^{k+1} c_i^{\rho} S^{k+1-i} = \Pi - \beta \frac{S^{k+1} I^k}{N} - \mu_1 S^{k+1}, \tag{28}$$

$$\sum_{i=0}^{k+1} c_i^{\rho} I^{k+1-i} = \beta \frac{S^{k+1} I^{k+1}}{N} - (\delta + \alpha_1 + \mu_1 + \mu_2) I^{k+1}, \tag{29}$$

$$\sum_{i=0}^{k+1} c_i^{\rho} Q^{k+1-i} = \delta I^{k+1} - (\alpha_2 + \mu_1 + \mu_2) Q^{k+1}. \tag{30}$$

Therefore, we design the following recursive formulae for the presented fractional model (7) as

$$S^{k+1} = \frac{\Pi - \sum_{i=1}^{k+1} c_i^{\rho} S^{k+1-i}}{c_0^{\rho} + \beta I^k / N + \mu_1}, \qquad k = 0, 1, 2, \dots, \tag{31}$$

$$I^{k+1} = \frac{-\sum_{i=1}^{k+1} c_i^{\rho} I^{k+1-i}}{c_0^{\rho} - \beta S^{k+1}/N + (\delta + \alpha_1 + \mu_1 + \mu_2)}, \qquad k = 0, 1, 2, \dots, \tag{32}$$

$$Q^{k+1} = \frac{\delta I^{k+1} - \sum_{i=1}^{k+1} c_i^{\rho} Q^{k+1-i}}{c_0^{\rho} + (\alpha_2 + \mu_1 + \mu_2)}, \qquad k = 0, 1, 2, \dots, \tag{33}$$

where c_0^{ρ} and c_i^{ρ}'s are calculated using the following recursive formulae

$$c_0^{\rho} = h^{-\rho}, \qquad c_i^{\rho} = \left(1 - \frac{1+\rho}{i}\right) c_{i-1}^{\rho}, \qquad i = 1, 2, 3, \dots, \tag{34}$$

where h is the time step size.

The numerical analysis helps to decide the function of ρ in the spread and control of COVID-19 in the proposed fractional model (7). For this purpose, we give some illustrations of the suggested model using a finite-difference technique established by R.E. Mickens. Fig. 1 depicts the impact of arbitrary fractional-order ρ on each class's total number of persons. For different values of ρ, the dynamics of the model are simulated. When the value of ρ is reduced from 1, the number of susceptible and quarantine persons steadily decline. However, the number of infected persons also reduces and the curves for each of the individuals S, I and Q straighten, when the value of ρ drops from 1 to 0.7. It is noted that for $\rho = 1$, we were at the Corona free equilibrium state, when $\delta = 0.5$ and $\mathcal{R}_\circ = 0.6653$. At P°, the size of each population is reducing with the decrease of fractional order ρ from 1. When $\delta = 0.07$, $\mathcal{R}_\circ = 3.6441$ and $\rho = 1$, we analyzed that the subpopulations converge to the Corona endemic equilibrium state $P^* = (S^*, I^*, Q^*)$ as illustrated in Fig. 2. These are the same results presented in [20] for the integer case. When the value of ρ is reduced from 1, the number of susceptible and quarantine persons steadily increase. However, the population of infected people also increases and the curves for each of the individuals S, I and Q straighten, when the value of ρ drops from 1 to 0.7.

9.2 The Impact of Quarantine Policies on Populations

Another successful COVID-19 control technique is a quarantine program that involves isolation of confirmed infected patients. The aim was to use a long-term quarantine program to control the spread of COVID-19 from the real data of Saudi Arabia. A numerical approach presents multiple numerical simulations under various quarantine levels. This numerical study has produced more attractive and remarkable consequences to examine the stability pattern of COVID-19 by using the values of fractional-order $\rho = 0.6, 0.7, 0.8, 0.9$. All simulations take place over up to 500 days. Fig. 3 shows that when the level of quarantine is raised, the population of susceptible people grows but the number of infected people gradually reduces. From Fig. 4, it is observed that when the quarantine rate rises, the number of infected people reduces at first (see for $\delta = 0.07, 0.14$) and then grows (see for $\delta = 0.21$). In Figs. 5-6, it has been noticed that when the rate of quarantine increases, the number of susceptible people also increases. It is shown that when the level of quarantine rises, the population of infected people reduces first (see for $\delta = 0.07, 0.14$) and then grows (see for $\delta = 0.21$). According to the simulations, lowering the value of fractional-order ρ and raising the quarantine rate δ led to a significant drop in Corona infected individuals. It is also worth noting that when the value of ρ lowers and δ rises, the peak size of each class gradually decreases and eventually flattens towards the time axis. These findings indicate that a proper and efficient quarantine strategy should be implemented in the absence of vaccines until the pandemic is eradicated.

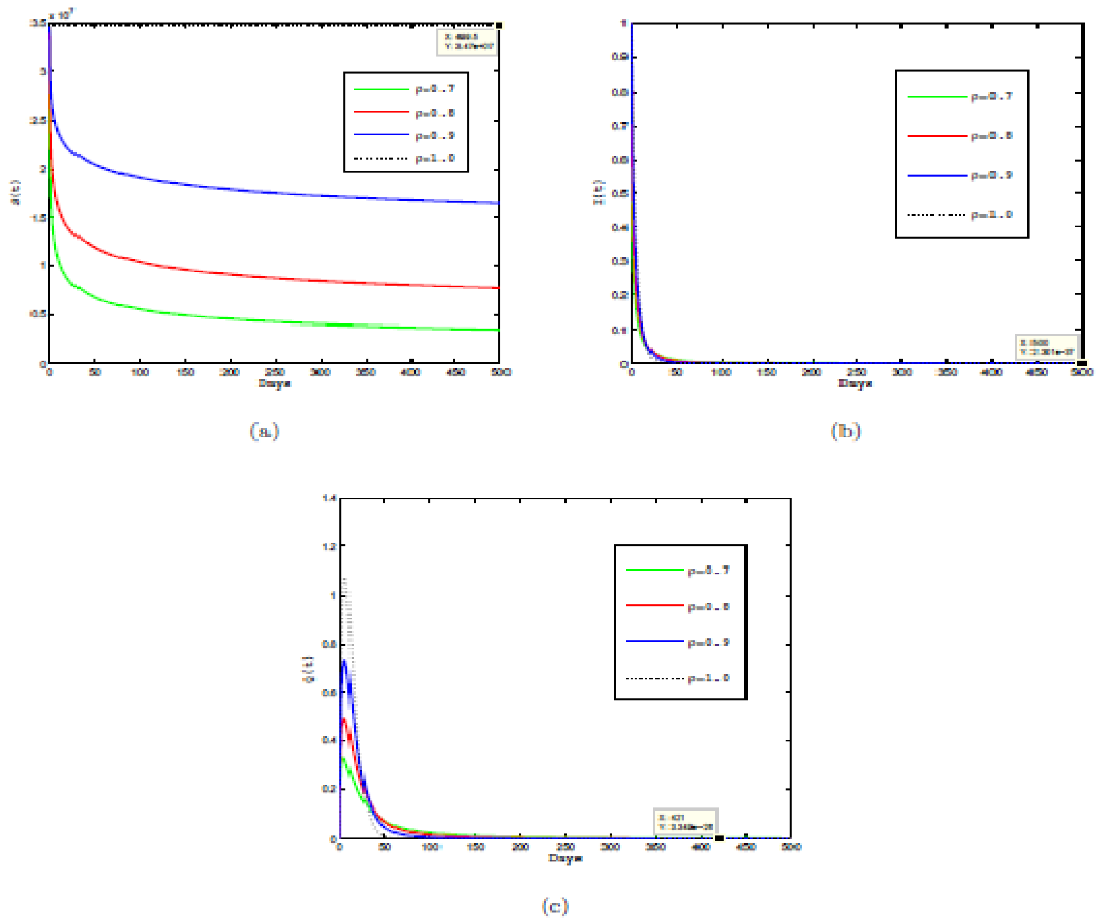

Figure 1: When the value of ρ is reduced from 1, the number of susceptible and quarantine persons steadily decline. However, the number of infected persons also reduces and the curves for each of the individuals S, I and Q straighten, when the value of ρ drops from 1 to 0.7.

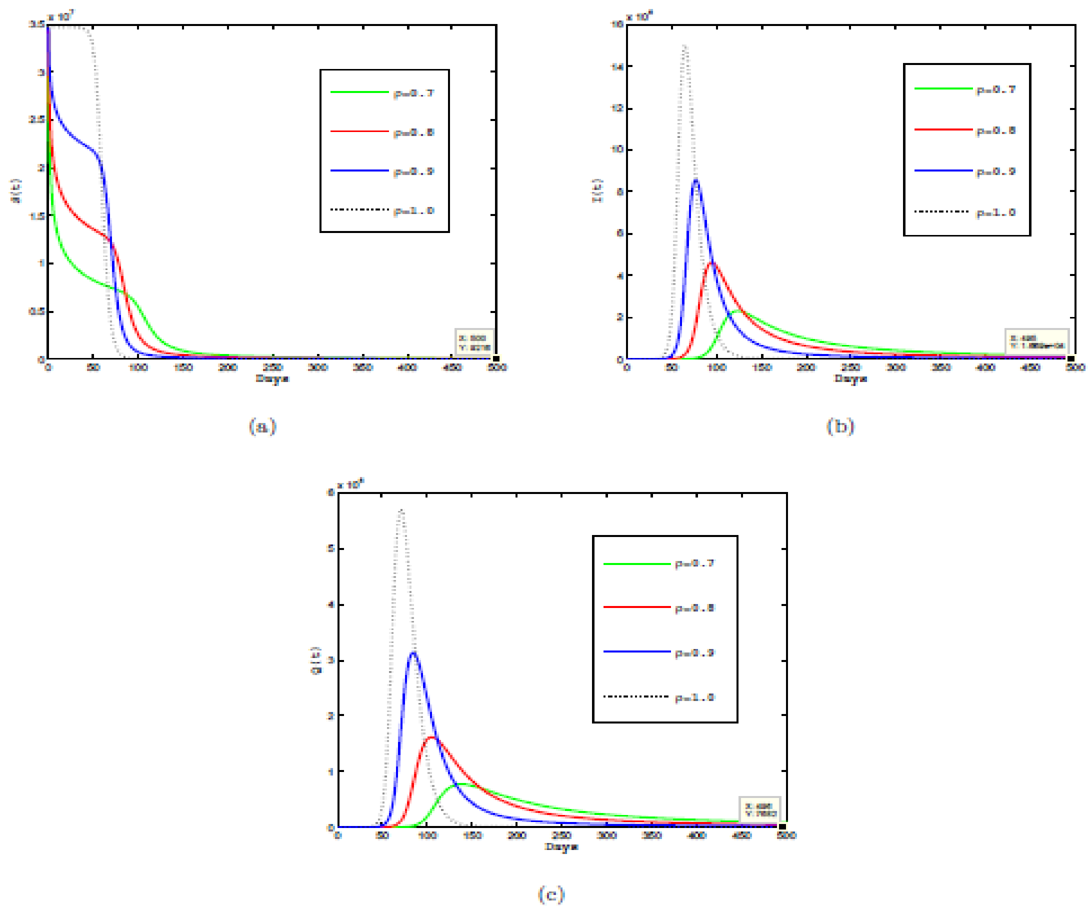

Figure 2: When the value of ρ is reduced from 1, the number of susceptible and quarantine persons steadily increase. However, the npopulation of infected people also increases and the curves for each of the individuals S, I and Q straighten, when the value of ρ drops from 1 to 0.7

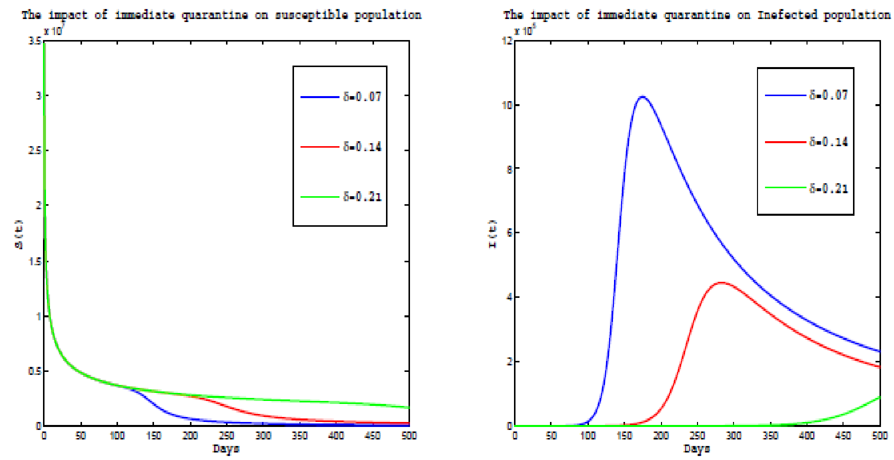

(a) (b)

Figure 3: For instance $\rho = 0.6$, the quarantine impact on the dynamics of the COVID-19 has been modelled. It has been noticed that when the level of quarantine is raised, the population of susceptible people grows but the number of infected people gradually reduces.

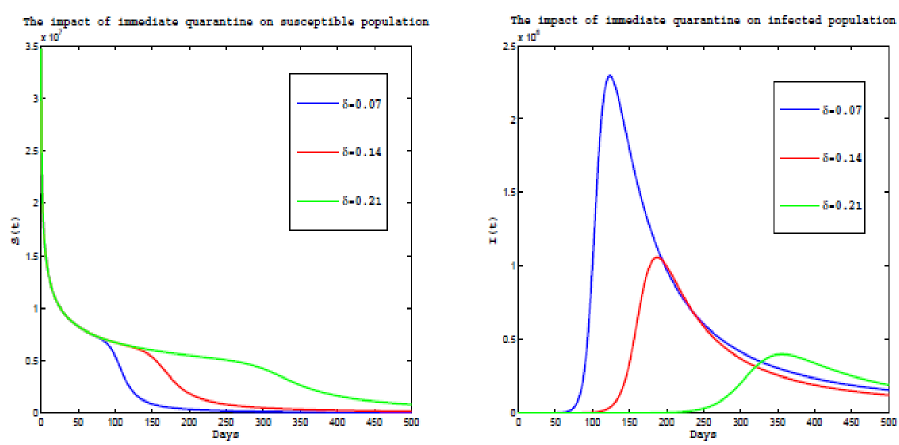

(a) (b)

Figure 4: For instance $\rho = 0.7$, the quarantine impact on the dynamics of the COVID-19 has been modelled. It has been noticed that when the rate of quarantine is raised, the number of susceptible people grows. It is worth noting that when the quarantine rate rises, the number of infected people reduces at first (see for $\rho = 0.07, 0.14$) and then grows (see for $\rho = 0.21$).

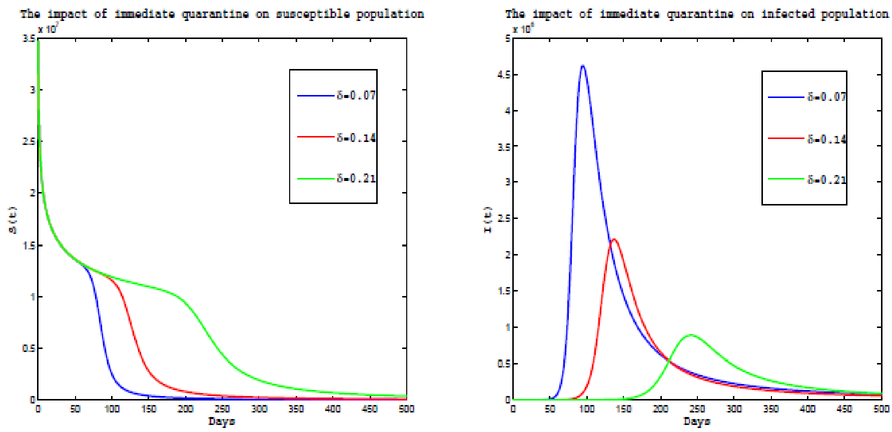

(a) (b)

Figure 5: For instance $\rho = 0.8$, the quarantine impact on the dynamics of the COVID-19 has been modelled. It has been noticed that when the rate of quarantine increases, the number of susceptible people also increases. It is shown that when the level of quarantine rises, the population of infected people reduces first (see for $\rho = 0.07, 0.14$) and then grows (see for $\rho = 0.21$).

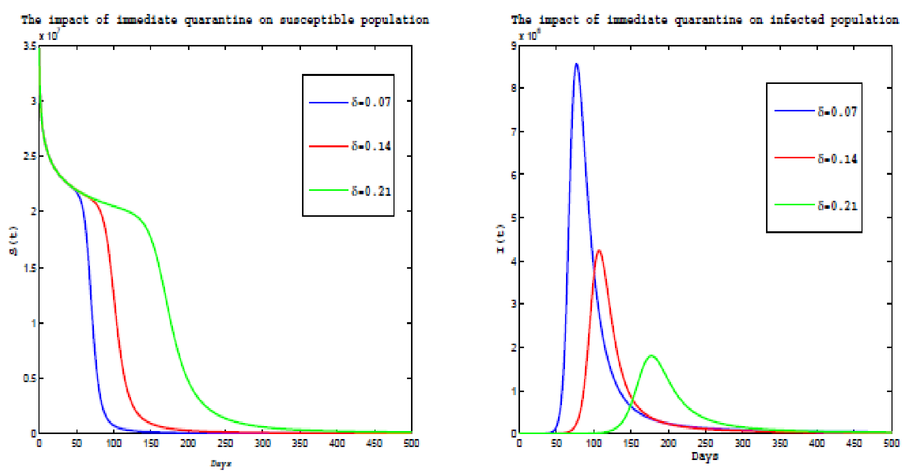

(a) (b)

Figure 6: For instance $\rho = 0.9$, the quarantine impact on the dynamics of the COVID-19 has been modelled. It has been noticed that when the rate of quarantine is raised, the number of susceptible people grows. It is important to note that when the period of quarantine rises, the population of infected people reduces at first (see for ρ=0.07, 0.14) and then increases (see for ρ=0.21).

10 Conclusions

Corona virus epidemic is being controlled primarily because of the quarantine program. Quarantine's influence on the disease dynamics has gained very little attention. Using a Caputo fractional model, we have investigated the transmission dynamics of the Corona virus disease with quarantine effects in this article. The model is initially defined using the ordinary differential equations, then reformed by employing the fractional operator. A mathematical analysis of the proposed fractional model has been done and the local stability has been proved for the Corona free and the Corona endemic cases. The basic reproduction number, the most significant threshold quantity, is described conceptually and quantitatively. To investigate the solution of the model, the NSFD numerical approach is employed from the literature. The results obtained from the numerical scheme are simulated and it is proved that they are compatible with the analytical results of the proposed model. Numerical illustrations have been used to show the Corona virus disease's long-term dynamical behavior. The main purpose was to see how various fractional-order ρ values affected the results. The fractional analysis shows that the population of susceptible people grows as the fractional order ρ falls. The infected and quarantine class sizes are reduced as the value of ρ decreases. Furthermore, COVID-19 declines gradually and managed by lowering the fractional-order ρ from 1. The results from the considered fractional model for the various values of ρ outperform the integer-order model. A second strategy has been presented to minimize the population of Corona infected cases by decreasing the fractional order ρ and increasing the quarantine level δ. Therefore, we concluded that could be eradicated a pandemic quickly if a human population implements obligatory quarantine measures at varying coverage levels while maintaining sufficient knowledge. Hence, the suggested SIQ fractional model is more efficient in fitting actual data than the SIQ integer-order model.

Conflicts of Interest The authors declare no conflict of interest.

References

[1] S. Agus & I. Darti (2021). On the nonstandard numerical discretization of SIR epidemic model with a saturated incidence rate and vaccination. *AIMS Mathematics*, *6*(1), 141–155. https://doi.org/10.3934/math.2021010.

[2] I. Ahmed, I. A. Baba, A. Yusuf, P. Kumam & W. Kumam (2020). Analysis of Caputo fractional-order model for COVID-19 with lockdown. *Advances in Difference Equations*, *2020*(1), Article number: 394. https://doi.org/10.1186/s13662-020-02853-0.

[3] M. I. Ahmed, M. Y. Hazlina & M. M. Rashid (2016). Mathematical modeling and control of active suspension system for a quarter car railway vehicle. *Malaysian Journal of Mathematical Sciences*, *10*(S), 227–241.

[4] A. Ali, M. Y. Khan, M. Sinan, F. M. Allehiany, E. E. Mahmoud, A. H. Abdel-Aty & G. Ali (2021). Theoretical and numerical analysis of novel COVID-19 via fractional order mathematical model. *Results in Physics*, *20*, Article number: 103676. https://doi.org/10.1016/j.rinp.2020.103676.

[5] M. Ali, S. T. H. Shah, M. Imran & A. Khan (2020). The role of asymptomatic class, quarantine and isolation in the transmission of COVID-19. *Journal of Biological Dynamics*, *14*(1), 389–408. https://doi.org/10.1080/17513758.2020.1773000.

[6] A. S. Alsheri, A. A. Alraeza & M. R. Afia (2022). Mathematical modeling of the effect of quarantine rate on controlling the infection of COVID19 in the population of Saudi Arabia. *Alexandria Engineering Journal*, *61*(9), 6843–6850. https://doi.org/10.1016/j.aej.2021.12.033.

[7] I. A. Baba & B. A. Nasidi (2021). Fractional order epidemic model for the dynamics of novel covid-19. *Alexandria Engineering Journal*, *60*(q), 537–548. https://doi.org/10.1016/j.aej.2020.09.029.

[8] D. Baleanu, S. Zibaei, M. Namjoo & A. Jajarmi (2021). A nonstandard finite difference scheme for the modeling and nonidentical synchronization of a novel fractional chaotic system. *Advances in Difference Equations*, *2021*, Article number: 308. https://doi.org/10.1186/s13662-021-03454-1.

[9] R. Begum, T. Osman, H. Khan, H. Gulzar & A. Khan (2021). A fractional order Zika virus model with Mittag-Leffler kernel. *Chaos, Solitons & Fractals*, *146*, Article number: 110898. https://doi.org/10.1016/j.chaos.2021.110898.

[10] C. Bekoe (2015). The SIR model and the 2014 ebola virus disease outbreak in Guinea, Liberia and Sierra Leone. *International Journal of Applied Sciences*, *6*(2), 11–24.

[11] Y. Belgaid, M. Helal, A. Lakmeche & E. Venturino (2021). A mathematical study of a coronavirus model with the Caputo fractional-order derivative. *Fractal and Fractional*, *5*(3), Article number: 87. https://doi.org/10.3390/fractalfract5030087.

[12] S. K. Choi, B. Kang & N. Koo (2014). Stability for Caputo fractional differential systems. *Abstract and Applied Analysis*, *2014*, Article ID 631419. https://doi.org/10.1155/2014/631419.

[13] D. Dwomoh, S. Iddi, B. Adu, J. M. Aheto, K. M. Sedzro, J. Fobil & S. Bosomprah (2021). Mathematical modeling of COVID-19 infection dynamics in Ghana: Impact evaluation of integrated government and individual level interventions. *Infectious Disease Modelling*, *6*, 381–397. https://doi.org/10.1016/j.idm.2021.01.008.

[14] H. Frank (1975). *Mathematical theories of populations: Demographics, genetics and epidemics*. Society for Industrial and Applied Mathematics Philapedia (SIAM), United States.

[15] Y. Guan, H. Chen, K. S. Li, S. Riley, G. M. Leung, R. Webster, J. S. M. Peiris & K. Y. Yuen (2007). A model to control the epidemic of H5N1 influenza at the source. *BMC Infectious Diseases*, *7*, Article number: 132. https://doi.org/10.1186/1471-2334-7-132.

[16] M. E. Hassan, H. Assoum, N. Bukharin, H. A. Otaibi, M. Mofijur & A. Sakout (2022). A review on the transmission of COVID-19 based on cough/sneeze/breath flows. *European Physical Journal Plus*, *137*(1), 1. https://doi.org/10.1140/epjp/s13360-021-02162-9.

[17] D. S. Hui (2020). The continuing 2019-nCoV epidemic threat of novel coronaviruses to global health - The latest 2019 novel coronavirus outbreak in Wuhan, China. *International Journal of Infectious Diseases*, *91*, 264–266. https://doi.org/10.1016/j.ijid.2020.01.009.

[18] D. S. Hui, E. I. Azhar, Y. J. Kim, Z. A. Memish, M. D. Oh & A. Zumla (2018). Middle east respiratory syndrome coronavirus: risk factors and determinants of primary, household, and nosocomial transmission. *The Lancet Infectious Diseases*, *18*(8), e217–e227. https://doi.org/10.1016/S1473-3099(18)30127-0.

[19] V. Iranzo & S. Pérez-González (2021). Epidemiological models and COVID-19: A comparative view. *History and Philosophy of the Life Sciences*, *43*(3), Article number: 104. https://doi.org/10.1007/s40656-021-00457-9.

[20] M. M. Khalsaraei, A. Shokri, S. Noeiaghdam & M. Molayi (2021). Nonstandard finite difference schemes for an SIR epidemic model. *Mathematics*, *9*(23), Article number: 3082. https://doi.org/10.3390/math9233082.

[21] H. Khan, F. Ahmad, T. Osman & M. Idrees (2022). On fractal-fractional Covid-19 mathematical model. *Chaos, Solitons & Fractals*, *157*, Article number: 111937. https://doi.org/10.1016/j.chaos.2022.111937.

[22] Y. Kim, A. V. Barber & S. Lee (2020). Modeling influenza transmission dynamics with media coverage data of the 2009 H1N1 outbreak in Korea. *PloS One*, *15*(6), Article ID: e0232580. https://doi.org/.

[23] S. R. Kumar & P. Sapra (2019). Fractional calculus and its applications for scientific professionals: A literature review. *International Journal of Modern Mathematical Sciences*, *17*(2), 111–137.

[24] L. O. Legesse & S. F. Balcha (2020). Optimal control strategies for the transmission risk of COVID-19. *Journal of Biological Dynamics*, *14*(1), 590–607. https://doi.org/10.1080/17513758.2020.1788182.

[25] H. Li, F. Y. Leong, G. Xu, C. W. Kang, K. H. Lim, B. H. Tan & C. M. Loo (2021). Airborne dispersion of droplets during coughing: A physical model of viral transmission. *Scientific Reports*, *11*, Article number: 4617. https://doi.org/.

[26] H. L. Li, L. Zhang, C. Hu, Y. L. Jiang & Z. Teng (2017). Dynamical analysis of a fractional-order predator-prey model incorporating a prey refuge. *Journal of Applied Mathematics and Computing volume*, *54*, 435–449. https://doi.org/10.1007/s12190-016-1017-8.

[27] D. Lokenath (2003). Recent applications of fractional calculus to science and engineering. *International Journal of Mathematics and Mathematical Sciences*, *2003*, Article ID 753601. https://doi.org/10.1155/S0161171203301486.

[28] Q. M. A. Mdallal, M. A. Hajji & T. Abdeljawad (2021). On the iterative methods for solving fractional initial value problems: New perspective. *Journal of Fractional Calculus and Nonlinear Systems*, *2*(1), 76–81. https://doi.org/10.48185/jfcns.v2i1.297.

[29] K. G. Mekonen, L. O. Legesse & T. G. Habtemichael (2022). Optimal control analysis for the coinfection of COVID-19 and TB. *Arab Journal of Basic and Applied Sciences*, *29*(1), 175–192. https://doi.org/10.1080/25765299.2022.2085445.

[30] E. Messina, M. Pezzella & A. Vecchio (2022). A non-standard numerical scheme for an age-of-infection epidemic model. *American Institute of Mathematical Sciences*, *9*(2), 239–252. https://doi.org/10.3934/jcd.2021029.

[31] J. Y. T. Mugisha, J. Ssebuliba, J. N. Nakakawa, C. R. Kikawa & A. Ssematimba (2021). Mathematical modeling of COVID-19 transmission dynamics in Uganda: Implications of complacency and early easing of lockdown. *PloS One*, *16*(2), Article number: e0247456. https://doi.org/10.1371/journal.pone.0247456.

[32] S. Murthy, C. D. Gomersall & R. A. Fowler (2020). Care for critically ill patients with COVID-19. *Journal of the American Medical Association*, *323*(15), 1499–1500. https://doi.org/10.1001/jama.2020.3633.

[33] P. A. Naik (2020). Global dynamics of a fractional-order SIR epidemic model with memory. *International Journal of Biomathematics*, *13*(8), Article number: 2050071. https://doi.org/10.1142/S1793524520500710.

[34] W. of Health Organization (2019). *Novel Coronavirus (2019- nCoV)*. https://www.who.int/emergencies/diseases/novel-coronavirus-2019.

[35] M. D. Ortigueira & D. Valério (2020). *Fractional signals and systems*. De Gruyter, Boston.

[36] M. A. A. Oud, A. Ali, H. Alrabaiah, S. Ullah, M. A. Khan & S. Islam (2021). A fractional order mathematical model for COVID-19 dynamics with quarantine, isolation, and environmental viral load. *Advances in Continuous and Discrete Models*, *2021*, Article number: 106. https://doi.org/10.1186/s13662-021-03265-4.

[37] W. Pan, T. Li & S. Ali (2021). A fractional order epidemic model for the simulation of outbreaks of Ebola. *Advances in Difference Equations*, *2021*(1), Article number:161. https://doi.org/10.1186/s13662-021-03272-5.

[38] D. Rajiv & J. Li (2020). Coughs and sneezes: Their role in transmission of respiratory viral infections, including SARS-CoV-2. *American Journal of Respiratory and Critical Care Medicine*, *202*(5), 651–659. https://doi.org/10.1164/rccm.202004-1263PP.

[39] U. A. M. Roslan & N. Y. Narayanan (2019). Sensitivity analysis for the dynamics of Leptospirosis disease. *Malaysian Journal Mathematical Sciences*, *13*(S), 77–84.

[40] J. S. H. Simon & J. F. T. Rabago (2018). Optimal control for a predator-prey model with disease in the prey population. *Malaysian Journal of Mathematical Sciences*, *12*(2), 269–285.

[41] J. S. H. Simon & J. F. T. Rabago (2018). Optimal control for a predator-prey model with disease in the prey population. *Malaysian Journal of Mathematical Sciences*, *12*(2), 269–285.

[42] B. R. Sontakke & A. S. Shaikh (2015). Properties of Caputo operator and its applications to linear fractional differential equations. *International Journal of Engineering Research and Applications*, *5*(5), 22–27.

[43] C. Tunç (2006). New results about stability and boundedness of solutions of certain non-linear third-order delay differential equations. *The Arabian Journal for Science and Engineering*, *36*(2), 185–196.

[44] C. Tunç (2010). Stability and bounded of solutions to non-autonomous delay differential equations of third order. *Nonlinear Dynamics*, *62*, 945–953. https://doi.org/10.1007/s11071-010-9776-5.

[45] C. Tunç & O. Tunç (2017). A note on the stability and boundedness of solutions to non-linear differential systems of second order. *Journal of the Association of Arab Universities for Basic and Applied Sciences*, *24*, 169–175. https://doi.org/10.1016/j.jaubas.2016.12.004.

[46] S. Vaz & D. F. M. Torres (2021). A dynamically-consistent nonstandard finite difference scheme for the SICA model. *Mathematical Biosciences and Engineering*, *18*(4), 4552–4571. https://doi.org/10.3934/mbe.2021231.

[47] S. Wang, W. Tang, L. Xiong, M. Fang, B. Zhang, C. Y. Chiu & R. Fan (2021). Mathematical modeling of transmission dynamics of COVID-19. *Big Data and Information Analytics*, *6*, 12–25. https://doi.org/10.3934/bdia.2021002.

[48] B. J. West (2017). *Nature's patterns and the fractional calculus*. De Gruyter, Boston.

[49] C. Xu, Z. Liu & C. Aouiti (2021). Further exploration on bifurcation of fractional-order six-neuron bi-directional associative memory neural networks with multi-delays. *Applied Mathematics and Computation*, *410*, Article number: 126458. https://doi.org/10.1016/j.amc.2021.126458.

[50] C. Y. Yang & J. Wang (2020). A mathematical model for the novel corona virus epidemic in Wuhan, China. *National Library of Medicine*, *17*(3), 2708–2724. https://doi.org/10.3934/mbe.2020148.

[51] B. G. Yazgaç & M. Kirci (2021). Fractional differential equation-based instantaneous frequency estimation for signal reconstruction. *Fractal and Fractional*, *5*(3), Article number: 83. https://doi.org/10.3390/fractalfract5030083.

[52] Z. U. A. Zafar, S. Younas, S. Zaib & C. Tunç (2022). An efficient numerical simulation and mathematical modeling for the prevention of tuberculosis. *International Journal of Biomathematics*, *15*(4), Aticle number: 2250015. https://doi.org/10.1142/S1793524522500152.

[53] Z. U. A. Zafar, S. Zaib, M. T. Hussain & C. Tunç (2022). Analysis and numerical simulation of tuberculosis model using different fractional derivatives. *Chaos Solitons Fractals*, *160*, Article number: 112202. https://doi.org/10.1016/j.chaos.2022.112202.

[54] A. Zeb, E. Alzahrani, V. S. Erturk & G. Zaman (2020). Mathematical model for coronavirus disease 2019 (COVID-19) containing isolation class. *BioMed Research International*, *2020*, Article ID 3452402. https://doi.org/10.1155/2020/3452402.

[55] Y. Zhou, Z. Ma & F. Brauer (2004). A discrete epidemic model for SARS transmission and control in China. *Mathematical and Computer Modelling*, *40*(13), 1491–1506. https://doi.org/10.1016/j.mcm.2005.01.007.